Dynamic Proteome Changes of *Shigella flexneri* 2a During Transition from Exponential Growth to Stationary Phase

Li Zhu[1], Xian-Kai Liu[1], Ge Zhao[1], Yi-Dan Zhi[1], Xin Bu[1], Tian-Yi Ying[1], Er-Ling Feng[1], Jie Wang[2], Xue-Min Zhang[2], Pei-Tang Huang[1]*, and Heng-Liang Wang[1]*

[1] *State Key Laboratory of Pathogen and Biosecurity, Beijing Institute of Biotechnology, Beijing 100071, China;* [2] *National Center of Biomedical Analysis, Beijing 100850, China.*

***Shigella flexneri* is an infectious pathogen that causes dysentery to human, which remains a serious threat to public health, particularly in developing countries. In this study, the global protein expression patterns of *S. flexneri* during transition from exponential growth to stationary phase *in vitro* were analyzed by using 2-D PAGE combined with MALDI-TOF MS. In a time-course experiment with five time points, the relative abundance of 49 protein spots varied significantly. Interestingly, a putative outer membrane protein YciD (OmpW) was almost not detected in the exponential growth phase but became one of the most abundant proteins in the whole stationary-phase proteome. Some proteins regulated by the global regulator FNR were also significantly induced (such as AnsB, AspA, FrdAB, and KatG) or repressed (such as AceEF, OmpX, SodA, and SucAB) during the growth phase transition. These proteins may be the key effectors of the bacterial cell cycle or play important roles in the cellular maintenance and stress responses. Our expression profile data provide valuable information for the study of bacterial physiology and form the basis for future proteomic analyses of this pathogen.**

Key words: *Shigella flexneri*, proteomics, growth phase

Introduction

Shigella species is a group of Gram-negative, non-spore forming, facultative pathogens closely related to *Escherichia coli*. The bacteria cause a disease called shigellosis in humans, an infection of the large intestine characterized by abdominal cramps, diarrhea, and fever. They can enter epithelial cells and trigger apoptosis in macrophages. There are four different species of *Shigella* based on the differences in O antigen and some biochemical reactions (*1*). Among them, *Shigella flexneri* is responsible for the majority of cases of endemic dysentery prevalent in developing countries where sanitation is poor. Most affected by this organism are children under five years old (*2*). Owing to the low infectious dose (10 to 100 bacteria) and the emergence of multiple resistance strains, knowledge about the physiology and pathogenesis of *Shigella* is urgently required.

***Corresponding authors.**
E-mail: wanghl@nic.bmi.ac.cn;
zhouxiaow@nic.bmi.ac.cn

The traditional bacterial life cycle has three phases, including lag phase, exponential or logarithmic phase, and stationary phase, while it can be expanded to include two additional phases: death phase and long-term stationary phase (*3*). The exponential phase is characterized by a period of population doublings, in which the cells consume nutrients and excrete waste products. The stationary phase is initiated as nutrient or toxic product concentrations reaching levels that can no longer support the maximum rate of growth. During transition from exponential growth to stationary phase, bacteria experience various environmental changes and their reproductive ability is gradually lost. However, the molecular mechanism underlying this trade-off between reproduction and survival has not been fully deciphered (*4*).

To investigate the physiology and molecular biology in a global scale during this transition, proteomic approaches have been applied in previous studies (*5*, *6*). In this study, we provide the profiles of phase-dependent proteins produced by *S. flexneri*

with high resolution and sensitivity. These data will expand our understanding of the question that how the whole proteome is regulated during the growth of this pathogen.

Results

Growth curve of *S. flexneri* 2a 2457T

The growth curve of *S. flexneri* serotype 2a strain 2457T in batch culture was constructed from the values of optical density OD_{600nm} as shown in Figure 1 (see Materials and Methods). We collected the bacteria and sampled for every 1 h from the exponential phase at OD_{600nm} of 0.6. The values of OD_{600nm} and the viability counts at each time point were measured (Table 1).

Protein expression profiles of *S. flexneri* 2a 2457T at different stages

Previous proteomic research of *S. flexneri* showed that most protein spots were scattered in the p*I* regions of pH 4–7 (*7*). Thus, our research also focused on the changes of acidic proteins at different stages.

As shown in Figure 2, the five two-dimensional polyacrylamide gel electrophoresis (2-D PAGE) gels of different stages are comparable with each other. More than 1,000 spots were detected on all of the five gels by Colloidal CBB staining. The total number of protein spots increased from Stages I to III, and then decreased from Stages IV to V. Some phase-specific proteins were almost not detected in Stage I or V. Most of the proteins whose expressions were continually induced or repressed and some of the proteins whose expressions fluctuated at different stages were cut out for further analysis. These protein spots are also indicated in Figure 2.

Identification and analysis of selected proteins

After destaining and in-gel trypsin digestion, a total of 49 spots representing 46 proteins were identified by matrix-assisted laser desorption/ionization time-of-flight mass spectrometry (MALDI-TOF MS). The database search results about these proteins are summarized in Table 2.

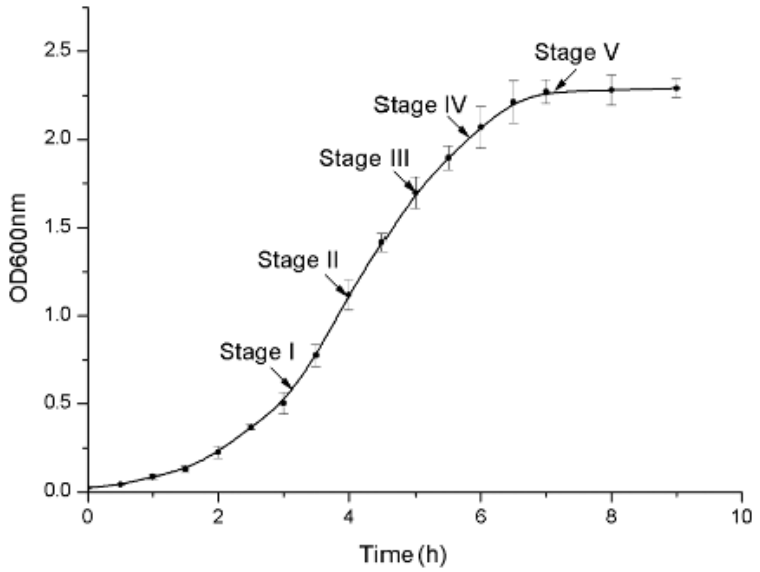

Fig. 1 The growth curve of *S. flexneri* 2a 2457T *in vitro* at 37°C. Arrows indicate the five time points (Stages I–V) at which the experiments were carried out.

Table 1 The values of OD_{600nm} and the viability counts at Stages I–V*

Stage	I	II	III	IV	V
OD_{600nm}	0.6	1.10±0.01	1.70±0.09	1.95±0.05	2.32±0.08
Viability counts (10^8 CFU)	1.54±0.14	2.35±0.29	5.67±0.99	12.8±1.20	16.07±1.56

*OD_{600nm}: optical density under 600 nm wavelength. CFU: colony forming units.

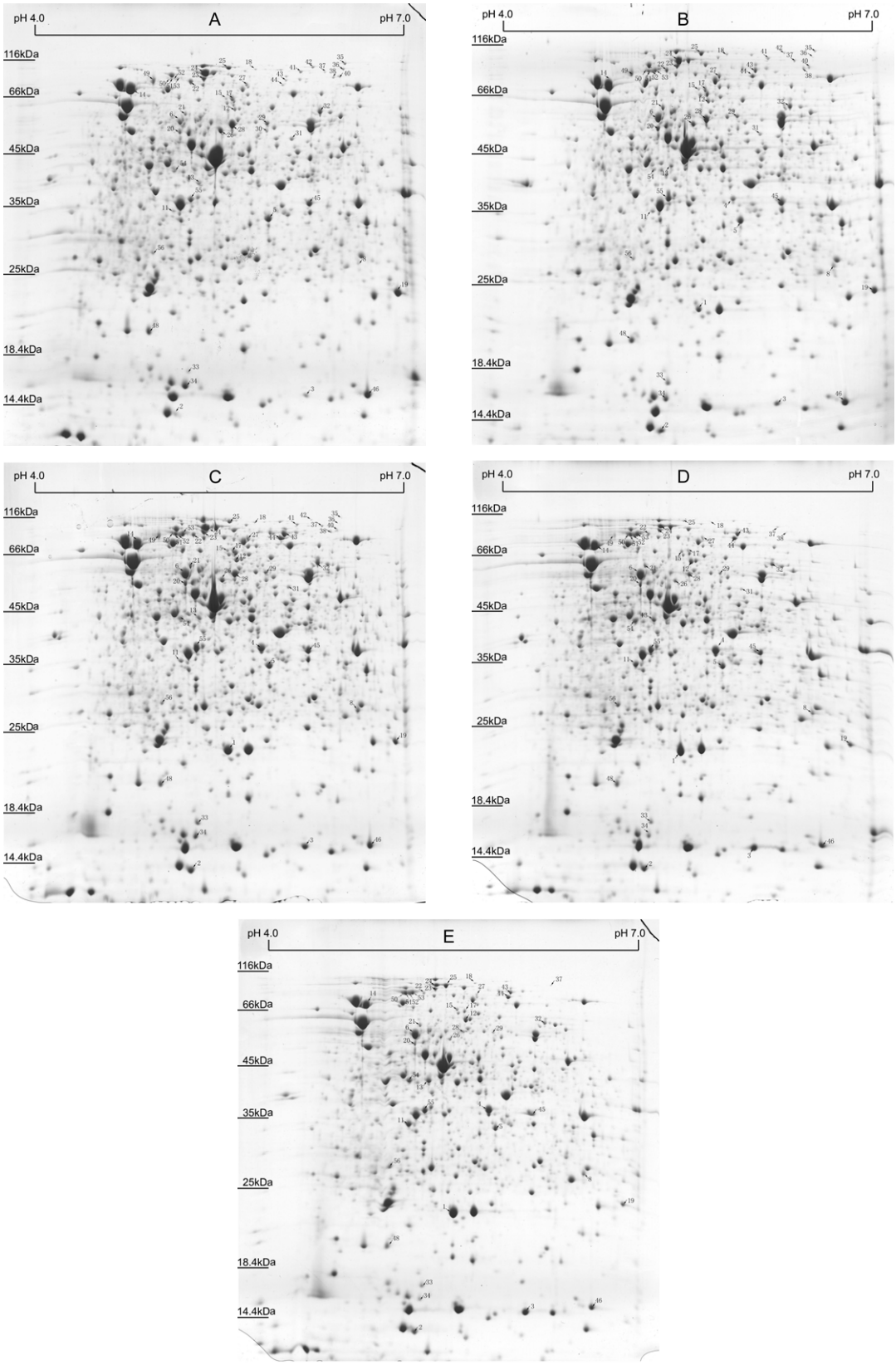

Fig. 2 Protein expression profiles of *S. flexneri* 2a 2457T at each growth stage. **A**–**E**: Stages I–V. Proteins were separated by IEF in the first dimension (18 cm) in the p*I* range of pH 4–7 and by 12.5% SDS-PAGE in the second dimension, and were detected by Coomassie-staining. Identified proteins were indicated by arrows and spot numbers (High-resolution graphs are available from authors upon request).

Table 2 Identification of 46 proteins by MALDI-TOF MS from *S. flexneri* 2a 2457T produced differentially at each growth stage

Spot No.	Protein symbol	Score	Accession No.	Locus ID	Sequence coverage	No. of matched peptides	Protein description
G01	YciD	69	gi|30062779	S1345	48%	10	putative outer membrane protein
G02	YfiD	129	gi|30063980	S2814	66%	11	putative formate acetyltransferase
G03	YnaF	70	gi|30062868	S1449	35%	9	putative filament protein
G04	AnsB	55	gi|30064278	S3157	29%	8	periplasmic L-asparaginase II
G05	FabI	176	gi|30062809	S1375	59%	20	enoyl-[acyl-carrier-protein] reductase (NADH)
G06	AspA	73	gi|30065514	S4560	22%	7	aspartate ammonia-lyase (aspartase)
G08	FrdB	86	gi|30065530	S4576	56%	12	fumarate reductase, iron-sulfur protein subunit
G11	MglB	66	gi|30063593	S2364	35%	9	galactose-binding transport protein
G12	PckA	58	gi|30065314	S4341	16%	6	phosphoenolpyruvate carboxykinase
G13	GlpQ	156	gi|30063673	S2454	76%	24	glycerophosphodiester phosphodiesterase
G14	RpsA	130	gi|30062446	S0971	39%	21	30S ribosomal subunit protein S1
G15	CpdB	103	gi|30065494	S4538	24%	11	2:3-cyclic-nucleotide 2-phosphodiesterase
G17	AspS	193	gi|30063276	S1942	44%	24	aspartate tRNA synthetase
G18	AlaS	59	gi|30064057	S2911	22%	12	alanyl-tRNA synthetase
G19	SodA	94	gi|30064799	S3763	58%	10	superoxide dismutase, manganese
G20	AsnS	201	gi|30062465	S0991	38%	18	asparagine tRNA synthetase
G21	GuaA	208	gi|30063899	S2725	40%	20	GMP synthetase (glutamine-hydrolyzing)
G22	YihK	150	gi|30064840	S3805	26%	14	putative GTP-binding factor
G23	Pta	223	gi|30063723	S2508	41%	25	phosphotransacetylase
G24	FusA	198	gi|30065374	S4404	52%	25	GTP-binding protein chain elongation factor EF-G
G25	AceE	246	gi|30061680	S0113	41%	30	pyruvate dehydrogenase (E1 component)
G26	SerS	98	gi|30062380	S0893	33%	13	serine tRNA synthetase
G27	Rnb	107	gi|30062807	S1373	28%	16	RNase II, mRNA degradation
G28	SucB	82	gi|30062110	S0583	24%	10	2-oxoglutarate dehydrogenase (E2 component)
G29	GltX	70	gi|30063801	S2605	24%	9	glutamate tRNA synthetase, catalytic subunit
G31	MrsA	147	gi|30064514	S3434	41%	16	putative phosphoglucomutase
G32	PykF	226	gi|30063190	S1838	59%	29	pyruvate kinase I
G33	OmpX	59	gi|30062298	S0807	35%	5	outer membrane protein X
G34	RpsF	61	gi|30065571	S4625	56%	9	30S ribosomal subunit protein S6
G35	SucA	143	gi|30062111	S0584	35%	27	2-oxoglutarate dehydrogenase (E1 component)
G36	Lon	255	gi|30061941	S0390	49%	34	DNA-binding, ATP-dependent protease La
G37	YhgF	99	gi|30065310	S4337	29%	14	hypothetical protein
G38	GlgB	91	gi|30065284	S4308	27%	17	1,4-alpha-glucan branching enzyme
G40	Prc	163	gi|30062914	S1511	39%	23	carboxy-terminal protease for penicillin-binding protein 3
G41	GyrB	162	gi|30065007	S4006	37%	21	DNA gyrase subunit B, type II topoisomerase
G42	NuoG	135	gi|30063709	S2494	31%	19	NADH dehydrogenase I chain G
G43	PflB	183	gi|30062438	S0962	40%	26	formate acetyltransferase 1
G44	FrdA	166	gi|30065531	S4577	49%	24	fumarate reductase, anaerobic, flavoprotein subunit
G45	CysK	192	gi|30063808	S2615	83%	24	cysteine synthase A, O-acetylserine sulfhydrolase A
G46	RplI	143	gi|30065574	S4628	73%	13	50S ribosomal subunit protein L9
G48	DksA	109	gi|30061705	S0140	76%	13	dnaK suppressor protein

Table 2 ***Continued***

Spot No.	Protein symbol	Score	Accession No.	Locus ID	Sequence coverage	No. of matched peptides	Protein description
G49	AceF	193	gi|30061681	S0114	51%	25	pyruvate dehydrogenase (E2 component)
G50	KatG	146	gi|30064765	S3727	33%	21	catalase; hydroperoxidase HPI(I)
G51	KatG	154	gi|30064765	S3727	36%	22	catalase; hydroperoxidase HPI(I)
G52	KatG	149	gi|30064765	S3727	36%	21	catalase; hydroperoxidase HPI(I)
G53	KatG	207	gi|30064765	S3727	48%	28	catalase; hydroperoxidase HPI(I)
G54	FucO	121	gi|30064145	S3008	46%	16	L-1,2-propanediol oxidoreductase
G55	OmpA	93	gi|30062494	S1023	52%	11	outer membrane protein 3a (II*;G;d)
G56	PurC	101	gi|30063855	S2669	59%	13	phosphoribosylaminoimidazole-succinocarboxamide synthetase, SAICAR synthetase

Bioinformatic analyses revealed that proteins involved in energy production and conversion (12/46) and translation (9/46) comprise a major part of the identified proteins. Others were related to cell wall or membrane biogenesis (4/46), carbohydrate metabolism (3/46), signal transduction (3/46), and so on. As to the subcellular localization, more than two thirds of these proteins were localized in cytoplasm. Besides, membrane proteins and periplasmic proteins were included, but only as a minor part. The detailed functional categories of these proteins based on the classification of Clusters of Orthologous Groups (http://www.ncbi.nlm.nih.gov/COG/) and the cellular localizations predicted by PSORTb v.2.0 (www.psort.org) were listed in Table 3. The relative abundance and expression patterns of identified proteins in the five gels at different stages were also described.

Table 3 Expression patterns and bioinformatic analyses of identified proteins

Spot No.	Protein symbol	Expression pattern*[1]	Relative abundance (volume)*[2]					COG*[3]	Localization
			Stage I	Stage II	Stage III	Stage IV	Stage V		
G01	YciD	↑↑↑↑	ND	0.338122	1.056830	1.431120	1.951640	M	Outer membrane
G02	YfiD	↑↑→↘	0.122546	0.360338	0.506921	0.518904	0.487855	R	Cytoplasm
G03	YnaF	↑↑↑↑	0.129985	0.243320	0.378834	0.649238	0.865560	T	Cytoplasm
G04	AnsB	↑↑↑↗	ND	0.191641	0.609328	0.911144	1.003750	–	Periplasmic space
G05	FabI	↓↘→↘	0.655974	0.507885	0.455764	0.437274	0.383020	I	Unknown
G06	AspA	↑↗↑↗	0.208366	0.807826	0.898268	1.145140	1.234040	E	Cytoplasm
G08	FrdB	↑↑↘↑	0.052497	0.107804	0.158431	0.143258	0.172969	C	Cytoplasm
G11	MglB	↑↑↑↑	0.045452	0.082542	0.105270	0.365603	0.521490	G	Periplasmic space
G12	PckA	↑↑↑↑	0.079557	0.140732	0.198588	0.257121	0.341101	C	Cytoplasm
G13	GlpQ	↑↑↑↑	0.088047	0.116600	0.156208	0.236151	0.372681	C	Periplasmic space
G14	RpsA	→↘↘↘	1.965550	1.884280	1.632840	1.422320	1.253910	J	Cytoplasm
G15	CpdB	↑↑↑↑	0.021617	0.028734	0.041985	0.056666	0.068310	F	Periplasmic space
G17	AspS	↓↑↓↓	0.183388	0.139781	0.192009	0.038185	ND	J	Cytoplasm
G18	AlaS	↑↓↓↓	0.012097	0.022594	0.013836	0.002166	ND	J	Cytoplasm
G19	SodA	↓↓↓↓	0.963829	0.518527	0.320438	0.252952	0.209230	P	Unknown
G20	AsnS	↑↘↘↓	0.143868	0.230065	0.199732	0.180855	0.134321	J	Cytoplasm
G21	GuaA	↑↓↗↘	0.073454	0.155249	0.100114	0.111852	0.095319	F	Cytoplasm
G22	YihK	↓→↓↘	0.160888	0.130163	0.126678	0.053317	0.047732	T	Cytoplasmic membrane
G23	Pta	↓↑↓↘	0.220020	0.162679	0.236062	0.173103	0.158659	C, R	Unknown
G24	FusA	↓↗↓↗	1.034700	0.856892	0.930851	0.326459	0.360715	J	Cytoplasm

Table 3 ***Continued***

Spot No.	Protein symbol	Expression pattern*[1]	Relative abundance (volume)*[2]					COG*[3]	Localization
			Stage I	Stage II	Stage III	Stage IV	Stage V		
G25	AceE	→↓↓↓	0.223033	0.228866	0.149161	0.024703	0.003513	C	Unknown
G26	SerS	↓↘↓↓	0.343742	0.251948	0.216105	0.093690	0.073963	J	Cytoplasm
G27	Rnb	↑↓↓↓	0.066073	0.109783	0.079980	0.042138	0.027965	–	Cytoplasm
G28	SucB	↓↓↓↓	0.802532	0.632209	0.516970	0.164995	0.100566	C	Cytoplasm
G29	GltX	↓↘↓↓	0.153128	0.103487	0.097153	0.053246	0.032579	J	Cytoplasm
G31	MrsA	↓↘↓↓	0.099794	0.063662	0.056220	0.032481	ND	G	Cytoplasm
G32	PykF	↓↘↓↓	0.286286	0.234922	0.199617	0.156574	0.114607	–	Unknown
G33	OmpX	↑↘↓↘	0.048283	0.189300	0.165548	0.129116	0.120927	M	Outer membrane
G34	RpsF	↓↓↓↓	0.574083	0.303693	0.219162	0.148161	0.099665	J	Cytoplasm
G35	SucA	↓↓↓ −	0.045815	0.021244	0.003809	ND	ND	C	Cytoplasm
G36	Lon	↓↓ −−	0.038085	0.004564	ND	ND	ND	O	Cytoplasm
G37	YhgF	↑↘↓↓	0.011495	0.021962	0.019492	0.011606	0.007427	K	Cytoplasm
G38	GlgB	↑↓↓↓	0.023470	0.036323	0.019335	0.006417	ND	G	Unknown
G40	Prc	↑↓↓ −	0.022055	0.032399	0.014425	ND	ND	M	Outer membrane
G41	GyrB	↓↓↓ −	0.056566	0.044323	0.031419	ND	ND	L	Cytoplasm
G42	NuoG	↓↓↓↓	0.041560	0.015792	0.006317	0.003104	ND	C	Unknown
G43	PflB	↑↑↓↓	0.023916	0.166535	0.357236	0.213656	0.156831	C	Cytoplasm
G44	FrdA	↑↑→→	0.024844	0.153955	0.268106	0.210036	0.216294	C	Periplasmic space
G45	CysK	↗↘↓↓	0.532310	0.579598	0.505064	0.396238	0.319571	E	Cytoplasm
G46	RplI	↓↓↘↘	0.948121	0.723898	0.531108	0.494982	0.456412	J	Cytoplasm
G48	DksA	↓↓↗↗	0.405237	0.322842	0.259510	0.279721	0.301116	T	Cytoplasm
G49	AceF	↓↓↓↓	0.241263	0.190662	0.142464	0.069324	ND	C	Cytoplasmic membrane
G50	KatG	↑↑↓↑	0.017953	0.042435	0.113385	0.091106	0.147822	P	Cytoplasm
G51	KatG	↑↑↑↑	0.003988	0.119471	0.188529	0.229915	0.324765	P	Cytoplasm
G52	KatG	↑↑↑→	0.011194	0.078571	0.112013	0.187740	0.188632	P	Cytoplasm
G53	KatG	↑↑↗→	0.034072	0.171998	0.236931	0.275466	0.283478	P	Cytoplasm
G54	FucO	↑↑↑↑	0.041224	0.078824	0.142970	0.279402	0.347836	C	Cytoplasm
G55	OmpA	↑↑↘→	0.312340	0.477371	0.670019	0.582806	0.593284	M	Outer membrane
G56	PurC	↓→↑↑	0.093432	0.077450	0.077493	0.188113	0.227420	–	Unknown

*[1]Ratio A is defined to represent the ratio of the relative abundance of one stage to its previous one, and Ratio B is defined to represent the ratio of the relative abundance of one stage to its next one. Then ↑ indicates Ratio A >1.2, ↓ indicates Ratio B >1.2, ↗ indicates Ratio A between 1.05 and 1.2, ↘ indicates Ratio B between 1.05 and 1.2, and → indicates Ratio A and Ratio B <1.05. *[2]The relative abundance of protein spot is represented by using the relative volume calculated. ND indicates that the protein spot was not detected in this stage. *[3]Each letter represents a particular functional category. These single letter codes can be decoded at the COG service (http://www.ncbi.nlm.nih.gov/COG/).

Discussion

Comparative genomics studies have shown that *S. flexneri* is closely related to *E. coli* and they might belong to the same genus based on DNA homology (*8*, *9*). Given the physiology research of *S. flexneri* is still limited, the features and functions of these proteins are mainly deduced from the information of homologous proteins in *E. coli*.

Carbon metabolism

From exponential growth to stationary phase, the available carbon resources in culture were gradually depleted. Carbon-starved bacterial cells were found to increase their synthesis of glycolysis enzymes, with a reduced production of tricarboxylic acid (TCA) cycle enzymes (*10*). The reaction catalyzed by pyruvate dehydrogenase is the gateway to the TCA cycle,

producing acetyl-CoA for the first reaction. The E1 (AceE, Spot G25) and E2 (AceF, Spot G49) components of this multienzyme complex were expressed decreasingly during the growth phase transition. The 2-oxoglutarate dehydrogenase is one of the key enzymes in the TCA cycle. The expression of E1 (SucA, Spot G35) and E2 (SucB, Spot G28) components of this multienzyme complex were also synchronally reduced in our experiments.

The expression of pyruvate-formate lyase (PflB, Spot G43), an enzyme critical in mixed acid fermentation, was significantly increased from Stages I to III, then decreased from Stages IV to V. Another putative pyruvate-formate lyase (YfiD, Spot G02) was expressed increasingly from Stages I to III, and then the amount of this protein maintained, just like the phenomenon observed in *E. coli* (*11*). These results supported the study that bacterial cells would convert their aerobic metabolism into anaerobic fermentation upon the stationary phase (*12*).

Respiratory electron acceptor

The fumarate reductase converts fumarate to succinate, acting as the key enzyme in fumarate respiration. We found that the expressions of fumarate reductase subunits A (FrdA, Spot G44) and B (FrdB, Spot G08) were induced during the growth phase transition. This indicated that cells of *S. flexneri* controlled their aerobic respiration and turned to use fumarate respiration to generate a proton gradient.

According to a previous report, fumarate is manufactured from C4-dicarboxylates and related compounds in Luria-Bertani (LB) medium, including oxaloacetate, malate, and aspartate (*13*). In our experiments, aspartase (AspA, Spot G06) and periplasmic asparaginase II (AnsB, Spot G04) were greatly induced. Therefore, AspA might have a role together with AnsB in the utilization of exogenous asparagine and the generation of fumarate. Accordingly, we can say, if aspartate (asparagine) was enough, the stationary accumulation of succinate might largely result from conversion of aspartate (asparagine) to fumarate via aspartase (and asparaginase), followed by reduction via fumarate reductase in fumarate respiration, although succinate could be produced through reductive branch of the TCA cycle pathway, which is the main pathway for succinate production in *Saccharomyces cerevisiae* during anaerobic glucose fermentation (*14*).

Oxidative defense machinery

Oxidation damage may be the Achilles's heel of stationary-phase bacterial cells, since many reported genes induced by stasis are related to the oxidative defense machinery (*4*, *15*). In our experiments, the expression of Mn-cofactored superoxide dismutase (SodA, Spot G19), which converts superoxide anions into molecular oxygen and hydrogen peroxide, was repressed. However, the bifunctional hydroperoxidase I (KatG, Spots G50–53), having both catalase and peroxidase activity, was induced greatly. This indicated that there were two different systems in the response of *S. flexneri* to the oxidation damage caused by reactive oxygen species, and KatG might play an important role in the stationary-phase oxidative defense machinery.

Interestingly, the KatG protein was identified in the present study as four separate spots (G50–53) with the same molecular weight but different isoelectric point values. This indicated that there might be two different modifications after translation for the two different functions of this enzyme, and there are two forms (reduced form and oxidated form) for each.

Translation-related proteins

The expressions of some ribosomal proteins were reduced during this transition, such as 50S ribosomal subunit protein L9 (RplI, Spot G46), 30S ribosomal subunit protein S6 (RpsF, Spot G34), and 30S ribosomal subunit protein S1 (RpsA, Spot G14). In the present study, we also identified some tRNA synthetases (or subunits), including aspartate tRNA synthetase (AspS, Spot G17), alanyl-tRNA synthetase (AlaS, Spot G18), asparagine tRNA synthetase (AsnS, Spot G20), serine tRNA synthetase (SerS, Spot G26), and glutamate tRNA synthetase catalytic subunit (GltX, Spot G29). The expression patterns of these proteins showed a trend of decreasing, although some fluctuating expressions existed. According to a previous report, the reduced production of proteins involved in translation might result from sigma factor competition (σ^S/σ^{70}) for RNA polymerase binding (*16*).

Outer membrane proteins

The protein with the most significant change in expression level is a putative outer membrane protein

YciD (OmpW, Spot G01), which could be seen as the hallmark of the stationary phase. A previous study showed that the protein is a receptor for Colicin S4 (*17*), but our data obviously suggested another role of this protein related to the growth of *S. flexneri*.

Then, a YciD null mutant strain was constructed by using the λ-phase Red recombination system (*18*). The mutant strain grew faster than wild-type strains in the liquid culture, and reached a higher final culture density. The colony diameter of the mutant strain was also bigger than wild-type strains. These primary results supported our hypothesis that the YciD protein controlled the growth of this pathogen. Furthermore, due to the polar localization of YciD (*19*), it might regulate the growth by changing the permeability of outer membrane.

Another outer membrane protein OmpA (Spot G55), which is one of the most abundant proteins in the outer membrane of *E. coli*, showed a trend of increasing in expression level. It was believed to form a nonspecific diffusion channel, allowing various small solutes to cross the outer membrane (*20*). In addition, the expression of protein OmpX (Spot G33) was reduced during the growth phase transition. The biological function of OmpX is still not clear, although the study on this protein has obtained some information recently (*21*). Interestingly, the targeting processes of OmpA and OmpX to the Sec-translocase for transport across the inner membrane were both SecB-dependent (*22*).

Other proteins

The expression of the universal stress protein YnaF (UspF, Spot G03) was dramatically induced during the growth phase transition. UspF has an adenine nucleotide-binding domain, and was found to be up-regulated under glucose limited conditions in a previous proteomic research of *E. coli* (*23*). Further analyses of this protein are now being processed.

Glycerophosphoryl diester phosphodiesterase (GlpQ, Spot G13) could hydrolyze deacylated phospholipids to an alcohol plus Glycerol-3-P that is subsequently transported into the cell and utilized as carbon sources. The expression of this enzyme was increasingly induced in our experiments. Thus, this protein might be involved in the stationary autophagy (dwarfing phenomenon), an important survival mechanism of bacteria (*4*).

The global regulator FNR

Many of the identified proteins (10/46) were under the control of the global transcriptional regulator FNR. Among these proteins, AceEF, NuoG, OmpX, SodA, SucAB, and YfiD were negatively regulated by FNR (*24*, *25*) and their expressions were reduced in our work; AnsB, AspA, FrdAB, and KatG were positively regulated by FNR (*24*, *25*) and their expressions were increased in our work. This is in agreement with the function of FNR. Therefore, the global transcriptional regulator FNR should play a key role in the growth phase transition.

Previous studies reported that the activity of FNR was regulated by oxygen. It would be active only during anaerobic growth and become inactivated even at very low O_2-tensions (1 μM) (*26*). Interestingly, our experiments were carried out at aerobic conditions. The expression changes of those proteins might be due to the decreasing amount of dissolved oxygen from exponential growth to stationary phase. Another possible explanation is that there is another defense mechanism to activate FNR (or another similar regulator?) for reducing the redox potential. This defense system would function at microaerobic stress conditions to protect the cell against potentially oxidative damages.

Benefiting from the high-resolution 2-D PAGE method, the majority of our results were coincident with those physiology phenomena reported previously. This global expression profiling research has revealed previously unrecognized relationships between different proteins and pathways in the life of *S. flexneri* 2a 2457T. These data provide a better understanding of the question that how protein production is regulated during the growth of this pathogen.

Materials and Methods

Preparation of whole-cell protein extract

A virulent *S. flexneri* serotype 2a strain 2457T was grown aerobically in 200 mL LB medium at 37°C. Cells were harvested at five time points from the exponential phase at an optical density OD_{600nm} of 0.6 till the bacteria grew into the stationary phase (represented as Stages I–V). The preparation of whole-cell protein extract was performed as described previously (*27*). The protein concentration of samples was measured by using the PlusOne 2-D Quant Kit

(Amersham Biosciences, Piscataway, USA), and 0.8 mg aliquots were stored at −80°C.

2-D PAGE

Isoelectric focusing (IEF) was performed by using immobilized pH gradient (IPG) strips (18 cm; Amersham Biosciences) at 20°C for 60,000 V·h. After IEF, each strip was equilibrated as described previously (*28*). For the second dimension, vertical slab sodium dodecyl sulfate (SDS)-PAGE (12.5%) was performed for about 4.5 h at 30 mA/gel by using a Bio-Rad Protean II Xi apparatus (Bio-Rad, Hercules, USA).

Image analysis was processed by ImageMaster 2D Platinum software (Amersham Biosciences), and the images of five stages (I–V) were compared. The relative volume of each spot was determined from the spot intensities in pixel units and normalized to the sum of the intensities of all the spots on the gel.

In-gel protein digestion and MALDI-TOF MS

The Coomassie-stained protein spots of interest were cut out, and in-gel protein digestion was performed as described previously (*28*). Peptides from digested proteins were resolubilized in 2 μL of 0.5% triflouroacetic acid (TFA). Peptide mass fingerprinting measurements were performed on a Bruker Reflex^{TM} III MALDI-TOF mass spectrometer (Bruker, Bremen, Germany) working in reflectron mode with 20 kV of accelerating voltage and 23 kV of reflecting voltage. A saturated solution of α-cyano-4-hydroxycinnamic acid in 50% acetonitrile and 0.1% TFA was used for the matrix. A total of 2 μL of the matrix solution and sample solution were mixed in a 1:1 (v/v) ratio and applied onto the Score 384 target well. The mass accuracy for peptide mass fingerprinting analysis was 0.1–0.2 Da with external calibration, and internal calibration was carried out by using enzyme autolysis peaks with the resolution of 12,000.

Protein identification

Database searches were performed by using the Mascot software (Matrix Science Ltd., London, UK) licensed in-house for the database of *S. flexneri* 2a 2457T (4,668 sequences) and checked again by using Mascot with free access on the Internet (www.matrixscience.com). Monoisotopic masses were used to search the databases, allowing a peptide mass error of 0.3 Da and one partial cleavage. Oxidation of methionine and carbamidomethyl modification of cysteine were considered. For unambiguous identification of proteins, more than five peptides must be matched, and the sequence coverage must be greater than 15%.

Acknowledgements

We thank Drs. Kai-Hua Wei and Jing Yuan for technical assistance and helpful discussion. This work was supported by the National Key Basic Research Program of China (973 Program, No. 2005CB522904) and the National Natural Science Foundation of China (No. 30470101).

Authors' contributions

LZ, YDZ, and XB carried out the 2-D PAGE experiments. LZ, XKL, and GZ performed the database search and bioinformatic analyses. TYY, ELF, and JW operated the MALDI-TOF MS instrument and calibrated all of the original MS data. XMZ contributed to the design and revision of this manuscript. HLW and PTH participated in the study design and helped to draft the manuscript. All authors read and approved the final manuscript.

Competing interests

The authors have declared that no competing interests exist.

References

1. Hale, T.L. 1991. Genetic basis of virulence in *Shigella* species. *Microbiol. Rev.* 55: 206-224.
2. Kotloff, K.L., *et al.* 1999. Global burden of *Shigella* infections: implications for vaccine development and implementation of control strategies. *Bull. World Health Organ.* 77: 651-666.
3. Finkel, S.E. 2006. Long-term survival during stationary phase: evolution and the GASP phenotype. *Nat. Rev. Microbiol.* 4: 113-120.
4. Nyström, T. 2004. Stationary-phase physiology. *Annu. Rev. Microbiol.* 58: 161-181.
5. Lee, K.J., *et al.* 2006. Proteomic analysis of growth phase-dependent proteins of *Streptococcus pneumoniae*. *Proteomics* 6: 1274-1282.

6. Wu, M., *et al.* 2005. The *Pseudomonas aeruginosa* proteome during anaerobic growth. *J. Bacteriol.* 187: 8185-8190.
7. Liao, X., *et al.* 2003. A two-dimensional proteome map of *Shigella flexneri*. *Electrophoresis* 24: 2864-2882.
8. Jin, Q., *et al.* 2002. Genome sequence of *Shigella flexneri* 2a: insights into pathogenicity through comparison with genomes of *Escherichia coli* K12 and O157. *Nucleic Acids Res.* 30: 4432-4441.
9. Wei, J., *et al.* 2003. Complete genome sequence and comparative genomics of *Shigella flexneri* serotype 2a strain 2457T. *Infect. Immun.* 71: 2775-2786.
10. Nyström, T. 1994. The glucose-starvation stimulon of *Escherichia coli*: induced and repressed synthesis of enzymes of central metabolic pathways and role of acetyl phosphate in gene expression and starvation survival. *Mol. Microbiol.* 12: 833-843.
11. Wyborn, N.R., *et al.* 2002. Expression of the *Escherichia coli* yfiD gene responds to intracellular pH and reduces the accumulation of acidic metabolic end products. *Microbiology* 148: 1015-1026.
12. Chang, D.E., *et al.* 2002. Gene expression profiling of *Escherichia coli* growth transitions: an expanded stringent response model. *Mol. Microbiol.* 45: 289-306.
13. Goh, E.B., *et al.* 2005. Hierarchical control of anaerobic gene expression in *Escherichia coli* K-12: the nitrate-responsive NarX-NarL regulatory system represses synthesis of the fumarate-responsive DcuS-DcuR regulatory system. *J. Bacteriol.* 187: 4890-4899.
14. Camarasa, C., *et al.* 2003. Investigation by ^{13}C-NMR and tricarboxylic acid (TCA) deletion mutant analysis of pathways for succinate formation in *Saccharomyces cerevisiae* during anaerobic fermentation. *Microbiology* 149: 2669-2678.
15. Potamitou, A., *et al.* 2002. Protein levels of *Escherichia coli* thioredoxins and glutaredoxins and their relation to null mutants, growth phase, and function. *J. Biol. Chem.* 277: 18561-18567.
16. Jishage, M., *et al.* 2002. Regulation of sigma factor competition by the alarmone ppGpp. *Genes Dev.* 16: 1260-1270.
17. Pilsl, H., *et al.* 1999. Characterization of colicin S4 and its receptor, OmpW, a minor protein of the *Escherichia coli* outer membrane. *J. Bacteriol.* 181: 3578-3581.
18. Murphy, K.C. and Campellone, K.G. 2003. Lambda Red-mediated recombinogenic engineering of enterohemorrhagic and enteropathogenic *E. coli*. *BMC Mol. Biol.* 4: 11.
19. Lai, E.M., *et al.* 2004. Proteomic screening and identification of differentially distributed membrane proteins in *Escherichia coli*. *Mol. Microbiol.* 52: 1029-1044.
20. Sugawara, E. and Nikaido, H. 1992. Pore-forming activity of OmpA protein of *Escherichia coli*. *J. Biol. Chem.* 267: 2507-2511.
21. Otto, K. and Hermansson, M. 2004. Inactivation of *ompX* causes increased interactions of type 1 fimbriated *Escherichia coli* with abiotic surfaces. *J. Bacteriol.* 186: 226-234.
22. Baars, L., *et al.* 2006. Defining the role of the *Escherichia coli* chaperone SecB using comparative proteomics. *J. Biol. Chem.* 281: 10024-10034.
23. Raman, B., *et al.* 2005. Proteome analysis to assess physiological changes in *Escherichia coli* grown under glucose-limited fed-batch conditions. *Biotechnol. Bioeng.* 92: 384-392.
24. Kang, Y., *et al.* 2005. Genome-wide expression analysis indicates that FNR of *Escherichia coli* K-12 regulates a large number of genes of unknown function. *J. Bacteriol.* 187: 1135-1160.
25. Salmon, K., *et al.* 2003. Global gene expression profiling in *Escherichia coli* K12. The effects of oxygen availability and FNR. *J. Biol. Chem.* 278: 29837-29855.
26. Unden, G., *et al.* 2002. Control of FNR function of *Escherichia coli* by O2 and reducing conditions. *J. Mol. Microbiol. Biotechnol.* 4: 263-268.
27. Yuan, J., *et al.* 2006. A proteome reference map and proteomic analysis of *Bifidobacterium longum* NCC2705. *Mol. Cell. Proteomics* 5: 1105-1118.
28. Ying, T., *et al.* 2005. Immunoproteomics of outer membrane proteins and extracellular proteins of *Shigella flexneri* 2a 2457T. *Proteomics* 5: 4777-4793.